Supporting Information

Efficiently Chemical Structure and Device Engineering for Achieving Difluorinated 2,2′-Bithiophene-Based Small Molecular Organic Solar Cells with 9.0% Efficiency

Min Li,[a] Zhongbin Qiu,[a] Guangjun Zhang,[c] Yu Liu,[a,b]* Lin Xiong,[a]

Dan Bai,[d] Mengbing Zhu,[b] Qiang Peng,[c]* Weiguo Zhu[b]*

[a] *College of Chemistry, Key Lab of Environment-Friendly Chemistry and Application in the Ministry of Education, Xiangtan University, Xiangtan 411105, China.*

[b] *School of Materials Science and Engineering, Jiangsu Engineering Laboratory of Light-Electricity-Heat Energy-Converting Materials and Applications, Jiangsu Collaborative Innovation Center of Photovoltaic Science and Engineering, National Experimental Demonstration Center for Materials Science and Engineering, Changzhou University, Changzhou 213164, China*

[c] *Key Laboratory of Green Chemistry and Technology of Ministry of Education, College of Chemistry, and State Key Laboratory of Polymer Materials Engineering, Sichuan University, Chengdu 610065, China*

[d]*Department of Biochemistry and Molecular Biology, School of Medicine, Xi'an Jiaotong University Xi'an, Shaanxi Province 710061, China*

*Email addresses:

(W, Z) zhuwig18@126.com

(Q. P) qiangpeng@scu.edu.cn

(Y. L) liuyu03b@126.com

Contents

1. Characterization and Measurement

Nuclear magnetic resonance (NMR) spectra were recorded on a Bruker AV-400 spectrometer using tetramethylsilane (TMS) as a reference in deuterated chloroform solution at 298 K. Mass spectrometric measurements were performed on Bruker Bifiex III MALDI-TOF. Thermogravimetric analyses (TGA) were conducted under a dry nitrogen gas flow at a heating rate of 20 $^{\circ}C$ min^{-1} on a Perkin-Elmer TGA 7. Differential scan calorimetry (DSC) measurements were carried out with a Netzsch DSC-204 under N_2 flow at heating and cooling rates of 10 °C min^{-1}. UV-Vis absorption spectra were recorded on a HP-8453 UV visible system. Cyclic voltammograms (CV) were carried out on a CHI660A electrochemical work station with a three electrode electrochemical cell in a 0.1 M tetrabutylammonium hexafluorophosphate ($TBAPF_6$) acetonitrile solution with a scan 100 mV s^{-1} at room temperature (RT) under argon atmosphere. In this three-electrode cell, a platinum rod, platinum wire and Ag/AgCl electrode were used as a working electrode, counter electrode and reference electrode, respectively. The surface morphology of the SMs:$PC_{71}BM$ blend film was investigated by an atomic force microscopy (AFM) on a Veeco, DI multimode NS-3D apparatus in a tapping mode under normal air condition at RT with a 5 μm scanner. The HOMO and LUMO distributions of SMs were calculated by the density functional theory (DFT) (B3LYP; 6-31G*) method.

2. ^{1}H NMR and ^{13}C NMR Spectra

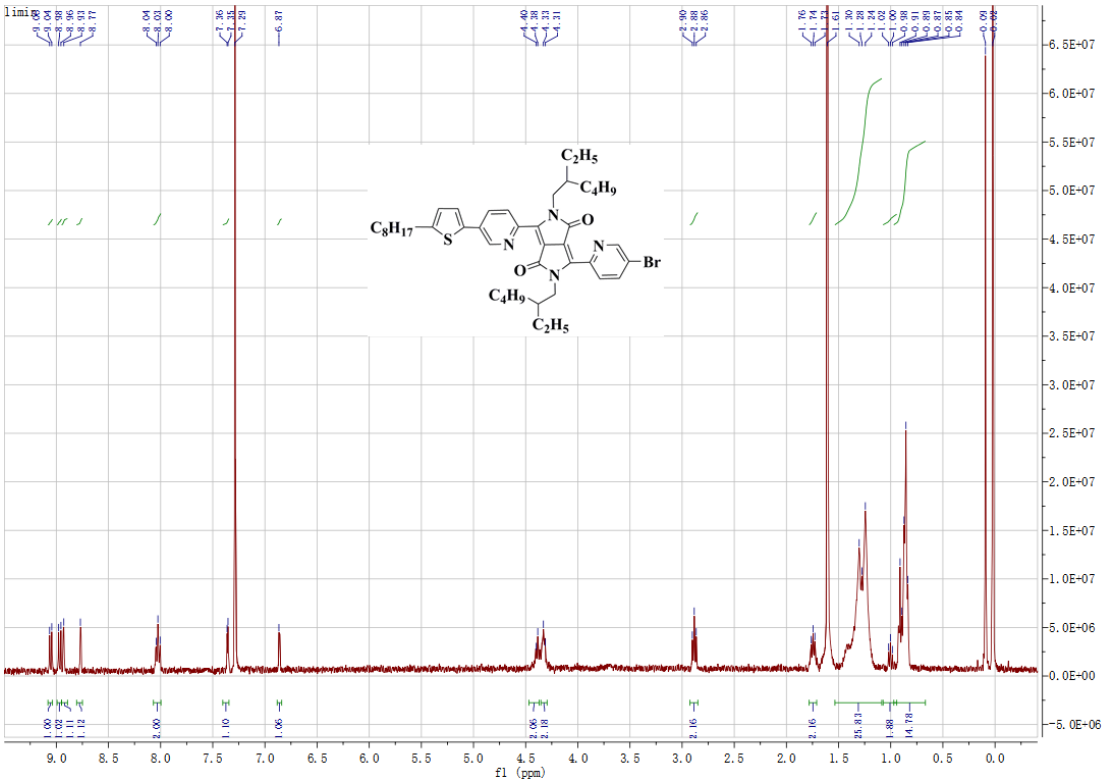

Fig.S1. ^{1}H NMR spectrum of BrPyDPP-TR$_1$

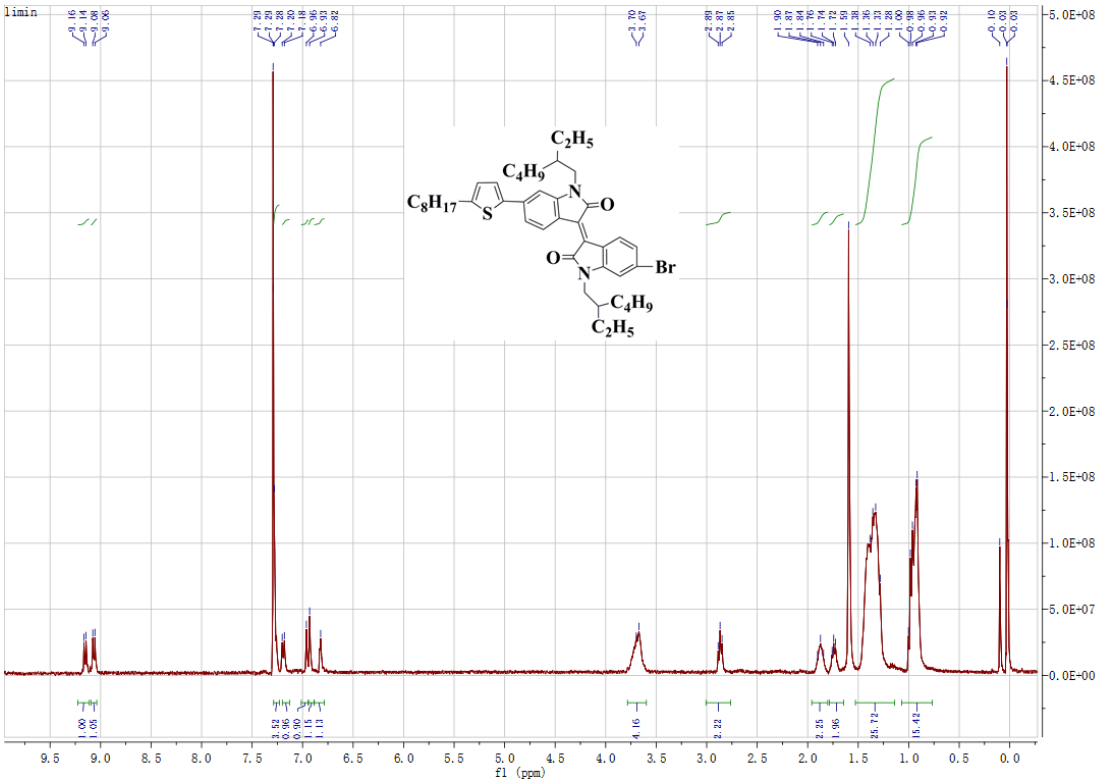

Fig. S2. ^{1}H NMR spectrum of BrIID-TR$_1$

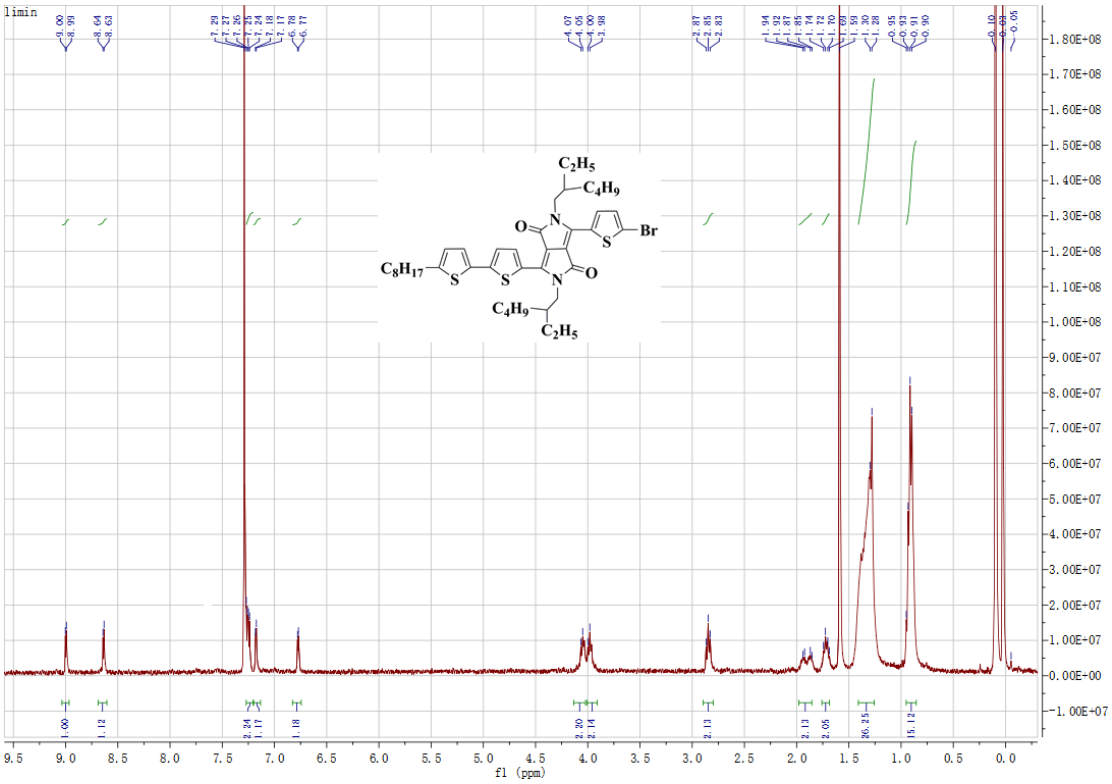

Fig.S3. ^{1}H NMR spectrum of BrTDPP-TR$_1$

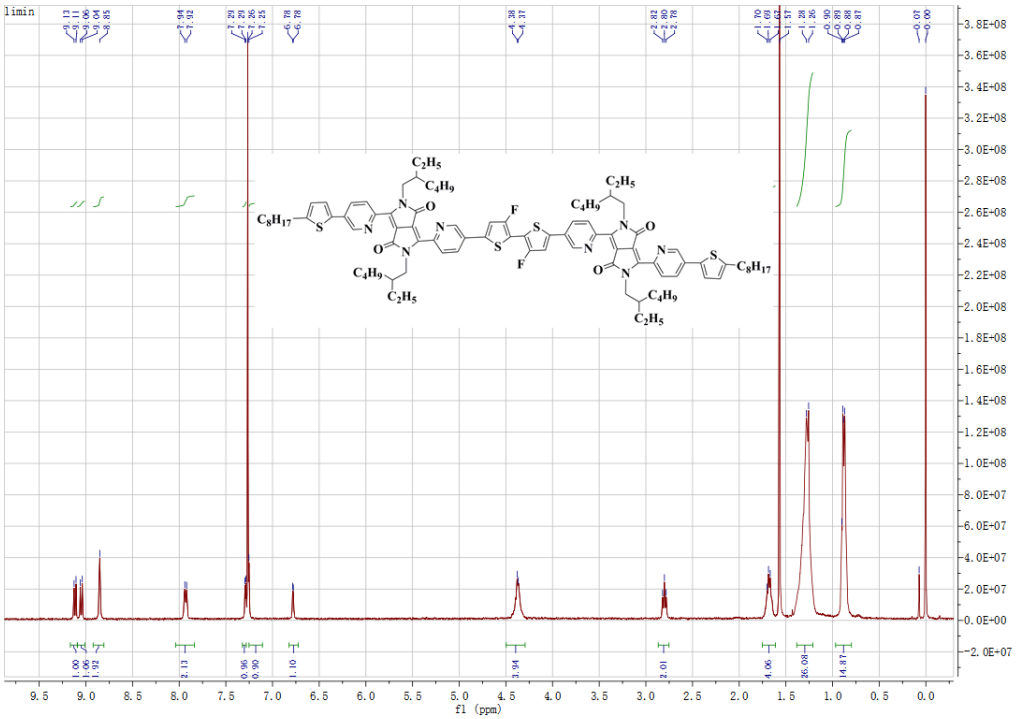

Fig. S4 ^{1}H-NMR spectrum of FBT(PyDPP-T)$_2$

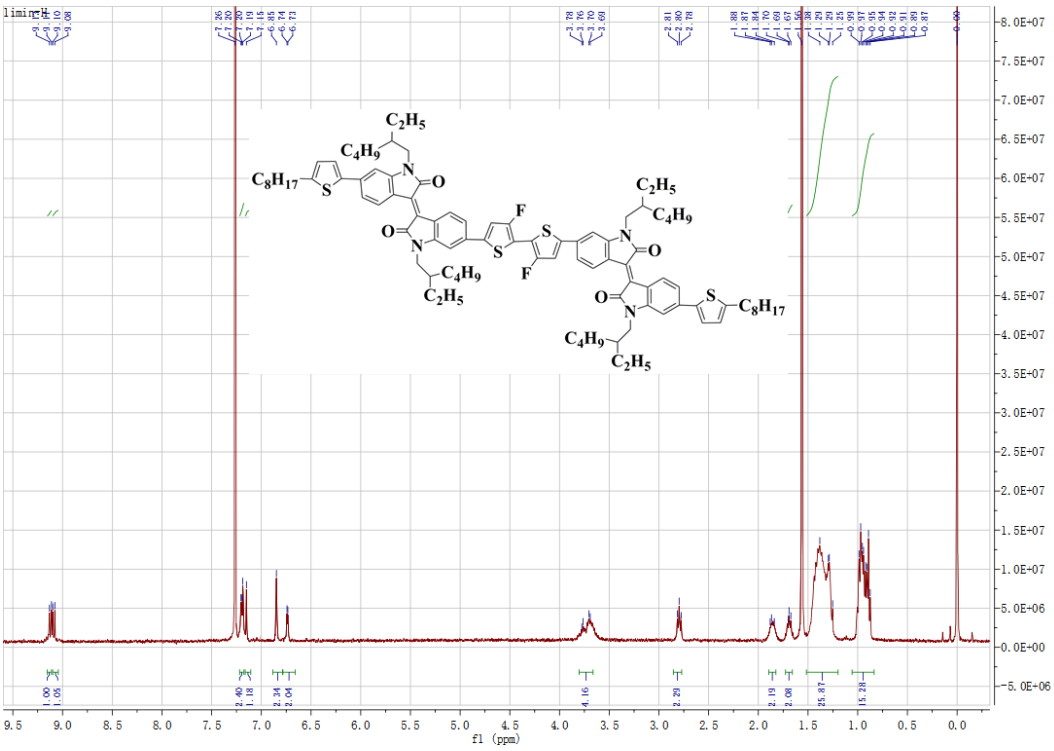

Fig. S5. ^{1}HNMR spectrum of FBT(TDPP-T)$_2$

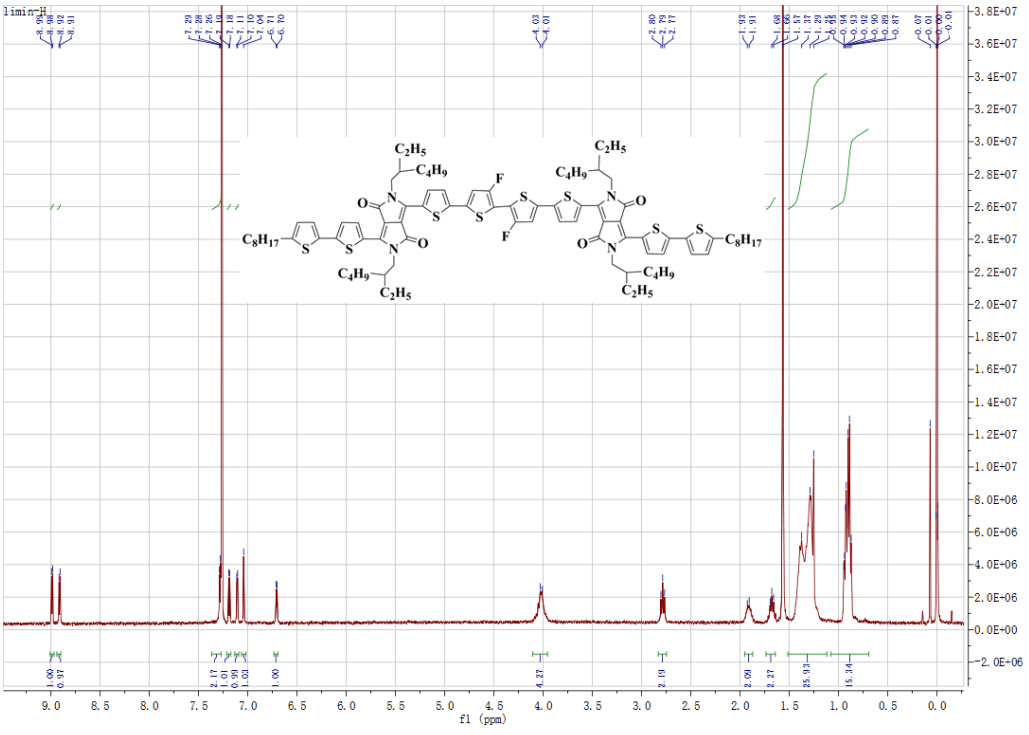

Fig. S6. ^{1}H-NMR spectrum of FBT(IID-T)$_2$

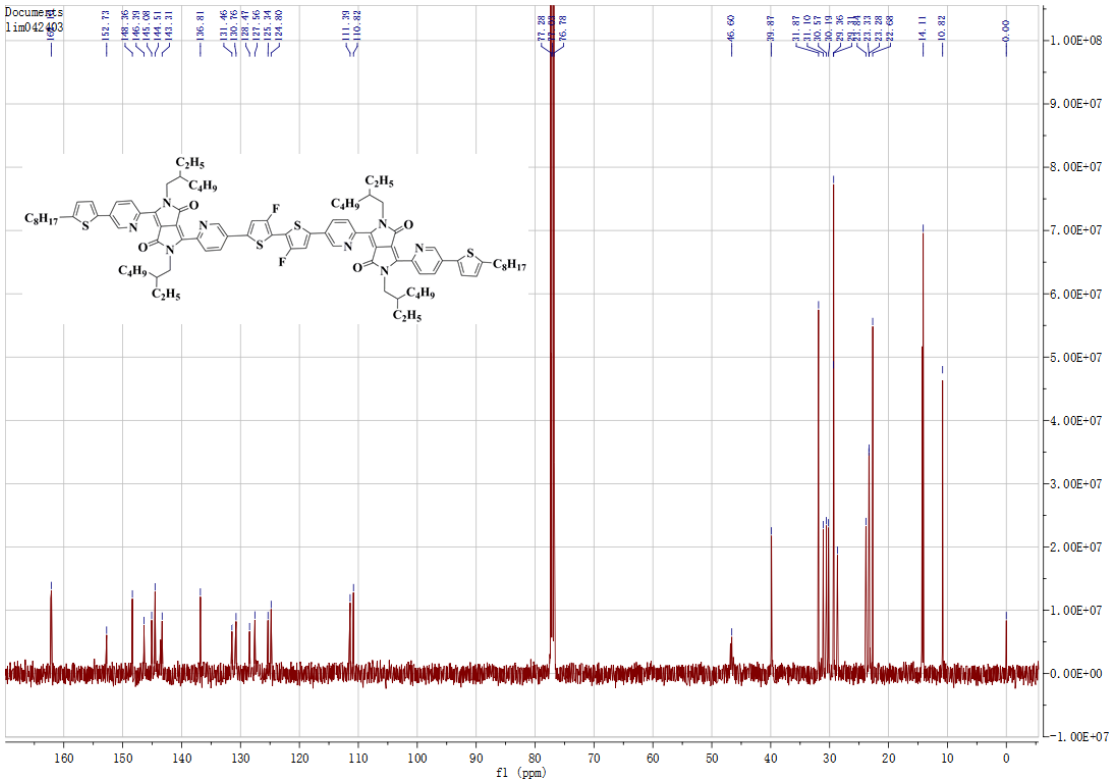

Fig. S7. ^{13}C-NMR spectrum of FBT(PyDPP-T)$_2$

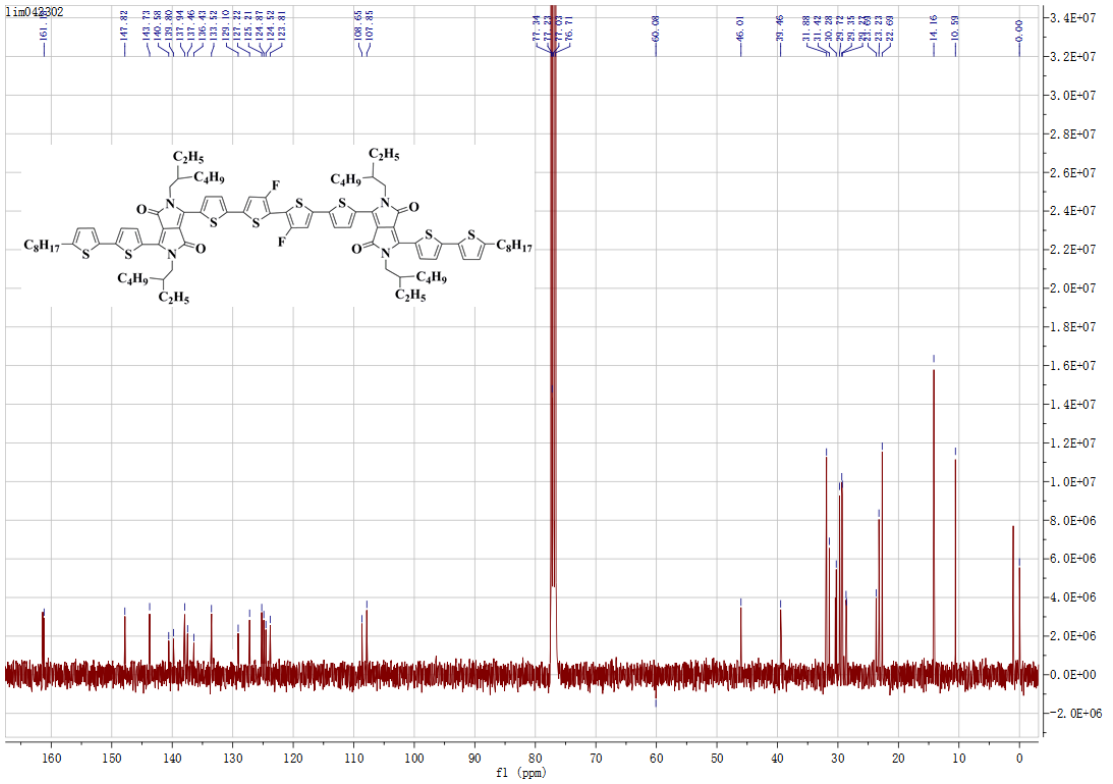

Fig. S8. ^{13}C-NMR spectrum of FBT(TDPP-T)$_2$

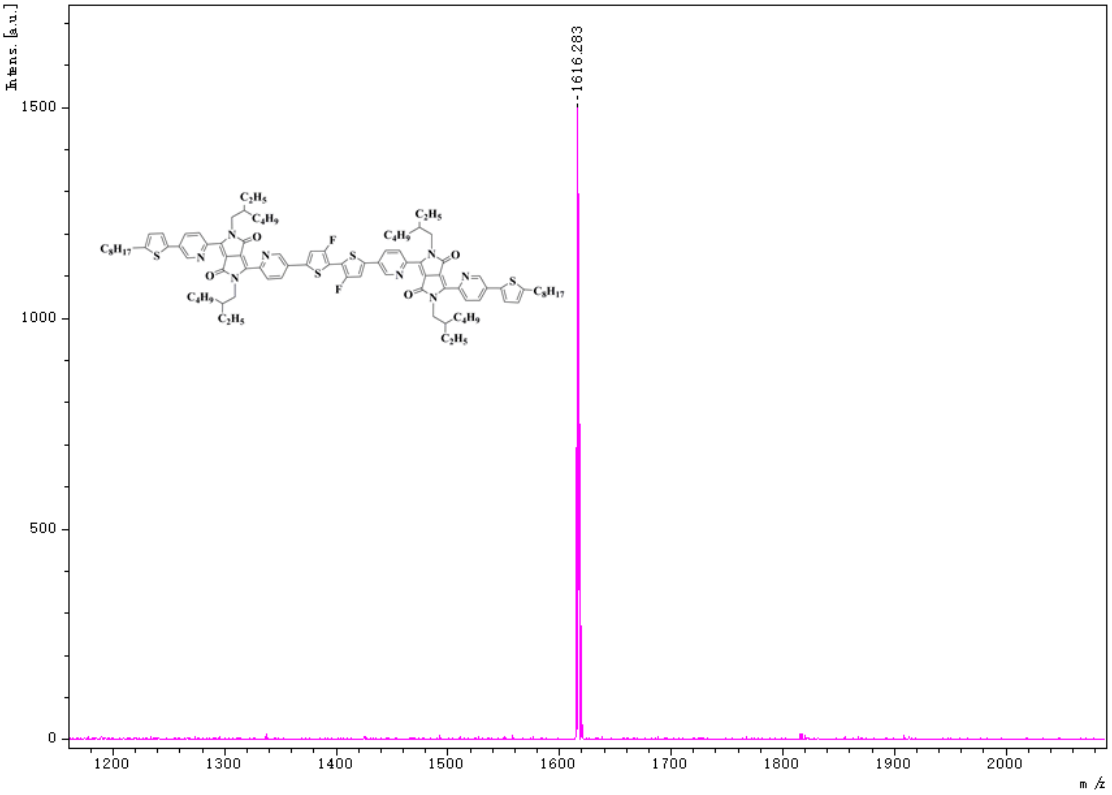

Fig. S9. MS spectrum of FBT(PyDPP-T)$_2$

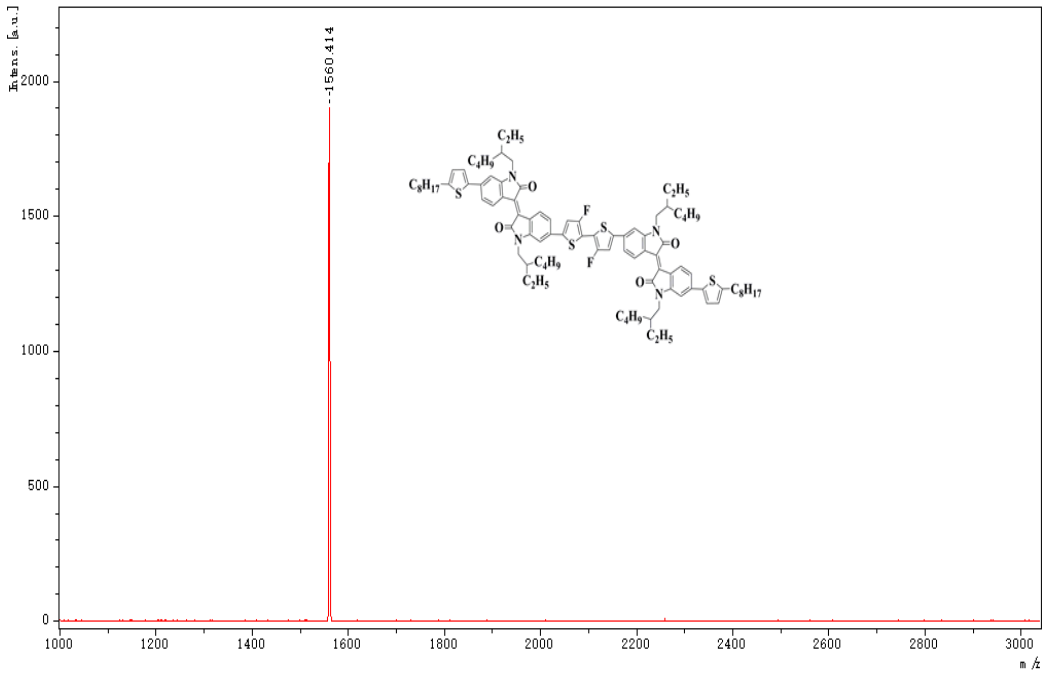

Fig.S10. MS spectrum of FBT(IID-T)$_2$

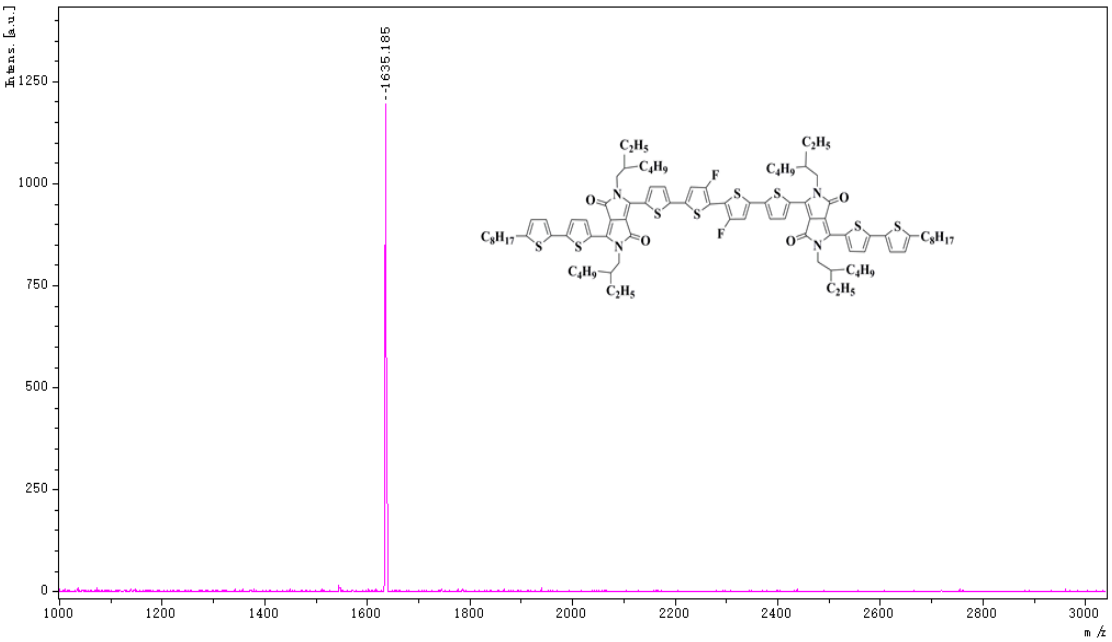

Fig. S11. MS spectrum of FBT(TDPP-T)$_2$

3. The absorption molar coefficient in different conditions.

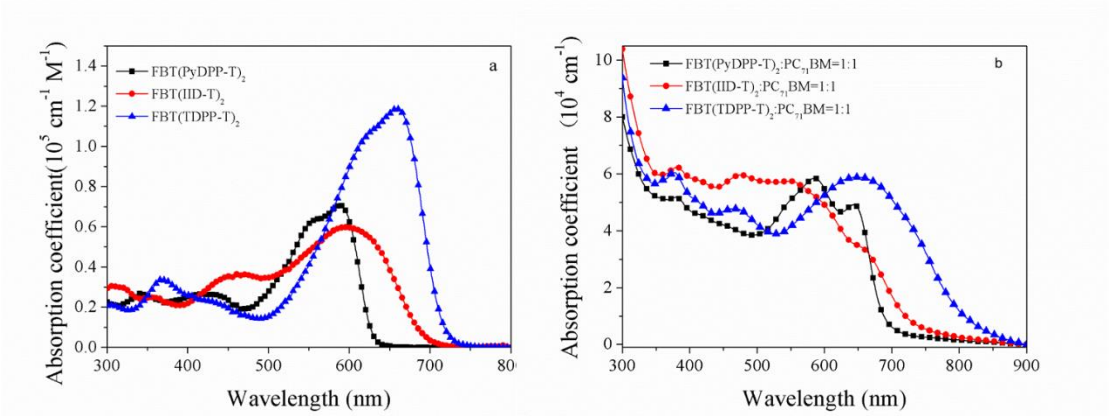

Fig.S12. Absorption spectra of SMs in a) dilute $CHCl_3$ and b) in their blend films with $PC_{71}BM$ at an optimized ratio of 1:1 (w/w), respectively.

4. Tauc plot of SMs to determine optical bandgap.

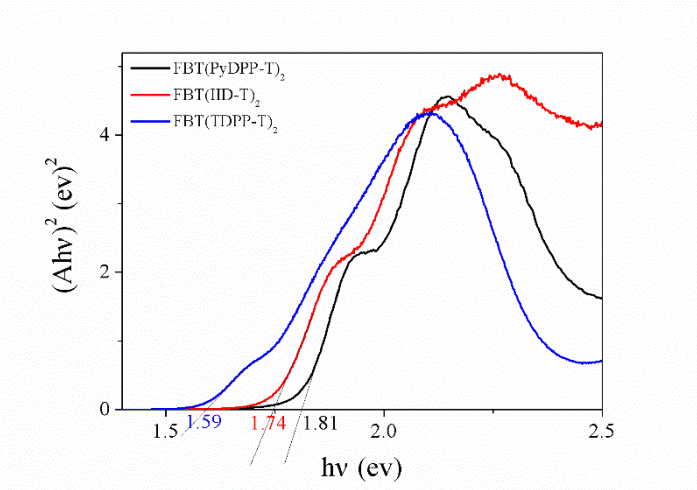

Fig.S13. Tauc plot of SMs to determine optical bandgap, from the equation of the related band gap E_g^{opt} and absorbance A: $(Ahν)^2 = B(hν - E_g^{opt})$.

5. Fabrication and Characterization of Organic Solar Cells

A sandwich structure of: ITO/PEDOT:PSS(5000 rpm, 140 °C 30min)/SM:$PC_{71}BM$ (2000 rpm)/Ca (10 nm)/Al (100 nm), was used in the solar cells. The photosensitive layer was subsequently prepared by spin-coating rate of 2000 rpm with a solution of the SM/$PC_{71}BM$ (1:1, *w/w*) at room temperature in chloroform (CF) with 0.4% CN (CN/CF, v/v) on the PEDOT:PSS layer with a typical concentration of 10 mg mL^{-1}, followed by CS_2-SVA treatment for 20 s. Ca (10 nm) and Al (100 nm) were successively deposited on the photosensitive layer in vacuum and used as top electrodes. The current-voltage (*I–V*) characterization of the devices was carried out on a computer-controlled Keithley source measurement system. A solar simulator was used as the light source and the light intensity was monitored by a standard Si solar cell. The active area was 0.1 cm^2 for each cell. The thicknesses of the spun-cast films were recorded by a profilometer (Alpha-Step 200, Tencor Instruments). The external quantum efficiency (*EQE*) was measured with a Stanford Research Systems model SR830 DSP lock-in amplifier coupled with WDG3 monochromator and a 150 W xenon lamp.

6. Photovoltaic properties of the FBT(PyDPP-T)$_2$/PC$_{71}$BM-based OPV cells.

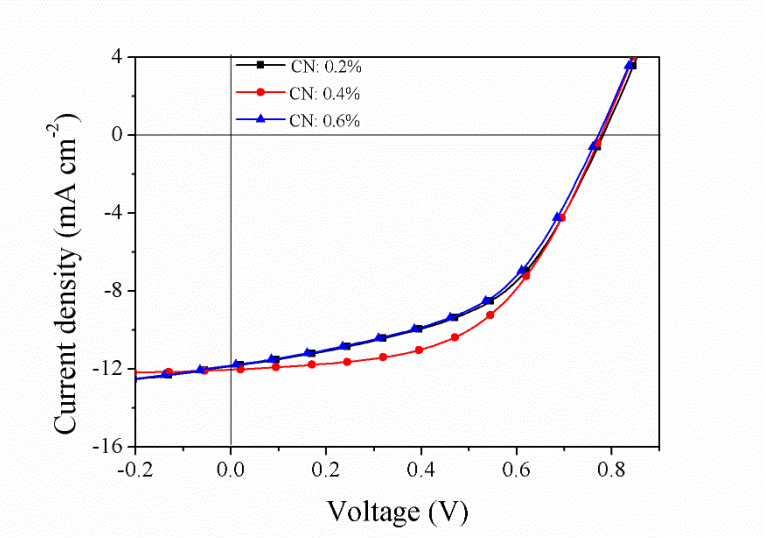

Fig. S14. *J-V* curve of the FBT(PyDPP-T)$_2$/PC$_{71}$BM-based OSCs under AM.1.5G illumination (100 mW/cm^2) with SM/PC$_{71}$BM CN ratios optimization.

Table S1. Photovoltaic parameters of the FBT(PyDPP-T)$_2$/PC$_{71}$BM-based PSCs under AM.1.5G illumination (100 mW/cm^2) with SM/PC$_{71}$BM CN ratios optimization.

CN	V_{oc} (V)	J_{sc} (mA/cm^2)	FF (%)	PCE (%)
0.2%	0.77	11.85	50.92	4.65(4.31)
0.4%	0.77	12.03	54.46	5.04(4.89)
0.6%	0.76	11.79	50.89	4.56(4.32)

Device condition:
(1) chloroform(CF)；
(2) concentration: 10 mg/mL of FBT(PyDPP-T)$_2$ in CF;
(3) Structure: ITO/PEDOT:PSS(5000 rpm, 140 ^{o}C 30min)/SM1:PC71BM (2000 rpm)/Ca (10 nm)/Al (100 nm).
(4) Spin-coating temperature： at room temperature.

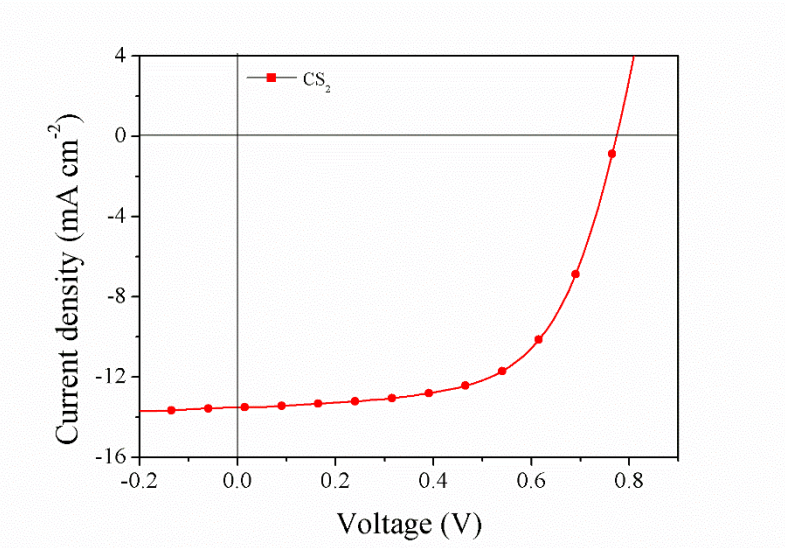

Fig. S15. *J-V* curve of the FBT(PyDPP-T)$_2$/PC$_{71}$BM-based SM-OSCs under AM.1.5G illumination (100 mW/cm^2) with CS_2 solvent anealing.

Table. S2. *J-V* curve of the FBT(PyDPP-T)$_2$/PC$_{71}$BM-based SM-OSCs under AM.1.5G illumination (100 mW/cm^2) with CS_2 solvent anealing.

Solvent	V_{oc}(V)	J_{sc} (mA/cm^2)	FF (%)	PCE (%)
CS_2	0.765	13.53	61.81	6.40(6.15)

Device condition:
(1) chloroform (CF);
(2) concentration: ITO/PEDOT:PSS(5000 rpm, 140 ^{o}C 30min)/SM1:PC$_{71}$BM (2000 rpm)/Ca (10 nm)/Al (100 nm)
(3) Solvent vapor annealing time: 20 s

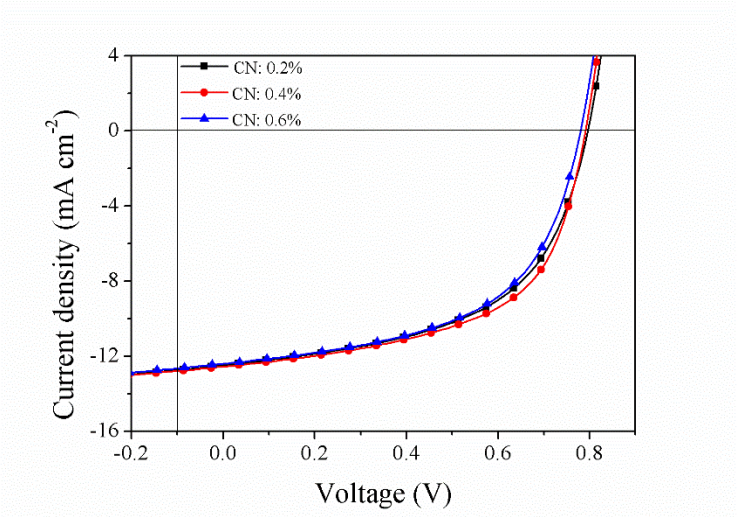

Fig. S16. *J-V* curve of the FBT(IID-T)$_2$/PC$_{71}$BM-based SM-OSCs under AM.1.5G illumination (100 mW/cm^2) with CN ratios optimization.

Table. S3. *J-V* curve of the FBT(IID-T)$_2$/PC$_{71}$BM-based SM-OSCs under AM.1.5G illumination (100 mW/cm^2) with CN ratios optimization.

CN	V_{oc} (V)	J_{sc} (mA/cm^2)	FF (%)	PCE (%)
0.2%	0.79	12.46	54.91	5.41(5.14)
0.4%	0.79	12.54	57.06	5.65(5.35)
0.6%	0.78	12.41	54.85	5.31(5.05)

Device condition:

(1) chloroform(CF)；

(2) concentration: 10 mg/mL of FBT(IID-T)$_2$ in CF;

(3) Structure: ITO/PEDOT:PSS(5000 rpm, 140 ºC 30min)/SM1:PC$_{71}$BM (2000 rpm)/Ca (10 nm)/Al (100 nm).

(4) Spin-coating temperature：at room temperature.

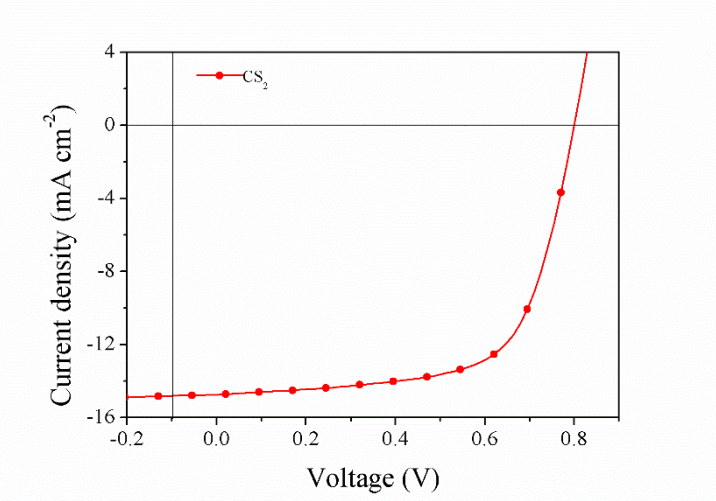

Fig. S17. *J-V* curve of the FBT(IID-T)$_2$/PC$_{71}$BM-based SM-OSCs under AM.1.5G illumination (100 mW/cm^2) with CS_2 solvent annealing.

Table. S4. *J-V* curve of the FBT(IID-T)$_2$/PC$_{71}$BM-based SM-OSCs under AM.1.5G illumination (100 mW/cm^2) with CS_2 solvent annealing.

Solvent	V_{oc} (V)	J_{sc} (mA/cm^2)	FF (%)	PCE (%)
CS_2	0.785	14.74	67.26	7.78(7.54)

Device condition:

(1) chloroform (CF);

(2) concentration: ITO/PEDOT:PSS(5000 rpm, 140 ºC 30min)/SM2:PC71BM (2000 rpm)/Ca (10 nm)/Al (100 nm)

(3) Solvent vapor annealing time: 20 s

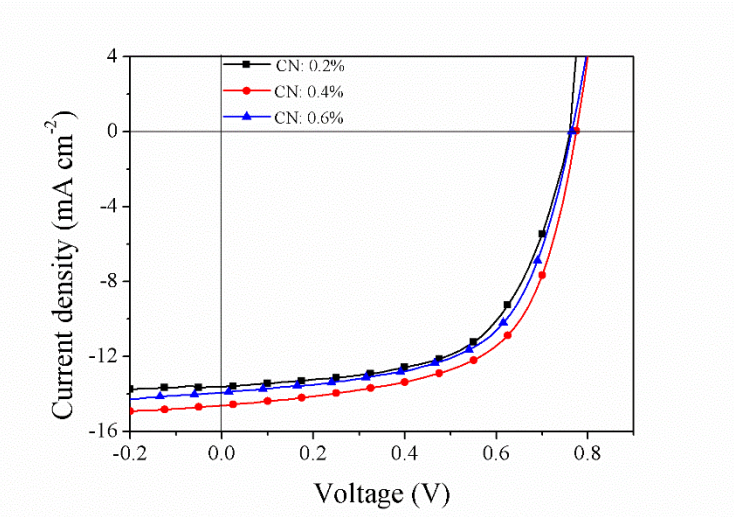

Fig. S18. *J-V* curve of the FBT(TDPP-T)$_2$/PC$_{71}$BM-based OSCs under AM.1.5G illumination (100 mW/cm^2) with SM/PC$_{71}$BM CN ratios optimization.

Table. S5. *J-V* curve of the FBT(TDPP-T)$_2$/PC$_{71}$BM-based SM-OSCs under AM.1.5G illumination (100 mW/cm^2) with CN ratios optimization.

CN	V_{oc} (V)	J_{sc}(mA/cm^2)	FF (%)	PCE (%)
0.2%	0.76	13.61	59.91	6.20(6.01)
0.4%	0.76	14.61	61.75	6.86(6.51)
0.6%	0.75	13.93	62.27	6.40(6.13)

Device condition:

(1) chloroform(CF)；

(2) concentration: 10 mg/mL of FBT(TDPP-T)$_2$ in CF;

(3) Structure: ITO/PEDOT:PSS(5000 rpm, 140 ºC 30min)/SM3:PC$_{71}$BM (2000 rpm)/Ca (10 nm)/Al (100 nm).

(4) Spin-coating temperature：at room temperature.

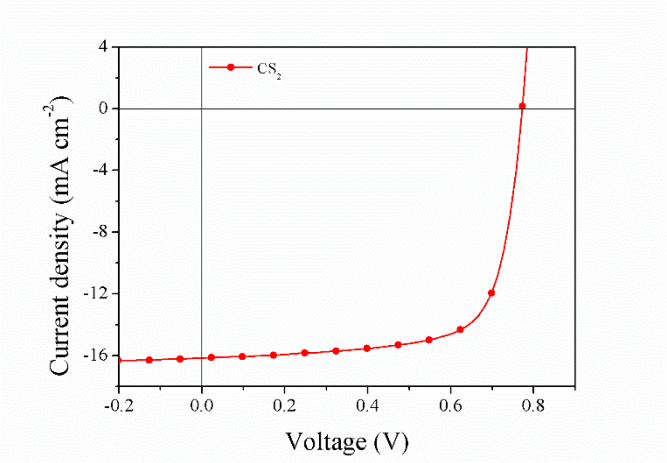

Fig. S19. *J-V* curve of the FBT(TDPP-T)$_2$/PC$_{71}$BM-based SM-OSCs under AM.1.5G illumination (100 mW/cm^2) with CS_2 solvent annealing.

Table. S6. *J-V* curve of the FBT(TDPP-T)$_2$/PC$_{71}$BM-based SM-OSCs under AM.1.5G illumination (100 mW/cm^2) with CS_2 solvent annealing.

Solvent	V_{oc} (V)	J_{sc} (mA/cm^2)	FF (%)	PCE (%)
CS_2	0.758	16.14	73.52	9.00(8.85)

Device condition:

(1) chloroform (CF);

(2) concentration: ITO/PEDOT:PSS(5000 rpm, 140 ºC 30min)/SM3:PC$_{71}$BM (2000 rpm)/Ca (10 nm)/Al (100 nm)

(3) Solvent vapor annealing time: 20 s